



Optimisation of artificial intelligence models and response surface methodology for predicting viscosity and relative viscosity of GNP-alumina hybrid nanofluid: incorporating the effects of mixing ratio and temperature

Adeola Borode¹ · Peter Olubambi¹

Accepted: 3 September 2023 / Published online: 21 September 2023
© The Author(s) 2023

Abstract

The viscosity properties of GNP-alumina hybrid nanofluids are of significant importance in various engineering applications. This study compares the predictive performance of response surface methodology (RSM), artificial neural network (ANN), and adaptive neuro-fuzzy inference system (ANFIS) for the viscosity (μ_{rel}) and relative viscosity (μ_{rel}) of GNP-alumina hybrid nanofluid at varying mixing ratio (0–3) and temperature (15–55 °C). The ANN and ANFIS models were optimised by varying the number and type of neurons and membership functions (MFs), respectively. In contrast, the RSM model was optimised by varying the source model. The efficacy of the models was assessed using various measures of performance metrics, including residual sum of squares, root mean square error, mean absolute error, and mean absolute percentage error (MAPE). The ANN architecture with 4 neurons exhibited exceptional proficiency in forecasting the μ_{nf} , achieving an R^2 value of 0.9997 and a MAPE of 0.3100. Meanwhile, the best ANN architecture for the μ_{rel} was achieved with 5 neurons, resulting in an R^2 of 0.9817 and MAPE of 0.2588. Furthermore, the ANFIS model with the difference of two sigmoidal MFs and the product of two sigmoidal MFs for μ_{nf} and Generalized Bell MFs for μ_{rel} exhibited the best performance with (3 5) and (4 5) input membership functions, respectively. An R^2 value of 0.9999 and 0.9872, with a corresponding MAPE value of 0.0945 and 0.1214, were reported for the optimal ANFIS architecture of μ_{nf} and μ_{rel} , respectively. The RSM model also produced its most accurate prediction with the quadratic model for both μ_{nf} and μ_{rel} , with an R^2 value of 0.9986 and 0.8835, respectively. Thus, comparative analysis across various models indicated that the ANFIS model outperformed others regarding performance metrics for both μ_{nf} and μ_{rel} . This study underscores the potential of ANN and ANFIS models in accurately forecasting the viscosity properties of GNP-alumina hybrid nanofluids, thus offering reliable tools for future applications.

Keywords Hybrid nanofluid · Graphene nanoplatelet · Alumina · Artificial neural network · Adaptive neuro-fuzzy inference system · Response surface methodology

List of symbols

2FI	2-Factor interaction
AI	Artificial intelligence
ANFIS	Adaptive neuro-fuzzy inference system
ANN	Artificial neural network
ANOVA	Analysis of variance
CI	Confidence interval
Coefficients $\alpha_0, \alpha_1, \alpha_2, \beta_0, \beta_1, \beta_2, \beta_3, \beta_4,$ $\beta_5, \gamma_0, \gamma_1, \gamma_2, \gamma_3, \gamma_4, \gamma_5, \gamma_6, \gamma_7, \gamma_8, \gamma_9$	Parameters of the regression equations for the RSM model
df	Degrees of freedom
DoE	Design of experiments
EG	Ethylene glycol
FCM-ANFIS	Fuzzy C-means adaptive neuro fuzzy inference system
Gauss2MF	Double gaussian membership function
GaussMF	Gaussian membership function
GbellMF	Generalised bell membership function
GNP	Graphene nanoplatelet
LR	Linear regression
MAE	Mean absolute error
MAPE	Mean absolute percentage error
MFs	Membership functions
MOD	Margin of deviation
MSE	Mean square error
n	Number of data points
PiMF	Pi-shaped membership function
PsigMF	Product of sigmas membership function
R	Correlation coefficient
R^2	Coefficient of determination
RMSE	Root mean square error
RSS	Residual sum of squares
RSM	Response surface methodology
SDS	Sodium dodecyl sulfate
SR	Shear rate
T	Temperature ($^{\circ}\text{C}$)
TrapMF	Trapezoidal membership function
TriMF	Triangular membership function
VIF	Variance inflation factor
φ	Nanoparticle volume fraction
μ	Viscosity (mPaS)
μ_i	Output of an artificial neuron

μ_{nf}	Viscosity of nanofluid
μ_{rel}	Relative viscosity of nanofluid

1 Introduction

The increasing demand for energy-saving solutions and the limited resources have highlighted the need for efficient heat transfer systems. Nanofluids have emerged as a promising solution due to their compelling heat transfer performance compared to traditional fluids, such as water, oil, and ethylene glycol (EG) [1]. The use of nanofluids has been gaining attention due to their remarkable properties and potential applications in various industries, particularly in enhancing heat transfer performance [2]. To further improve the properties of nanofluids, hybrid nanofluids have been studied, and they have shown more promising heat transfer enhancement effects than single nanofluids in most cases [3]. Numerous studies [3–5] have confirmed the potential of these nanofluids. Therefore, hybrid nanofluids are gaining attention as an effective solution to improve heat transfer efficiency, which can lead to energy savings and a reduction in greenhouse gas emissions. Further research on hybrid nanofluids is needed to optimise their properties and understand their behaviour under different conditions.

Hybrid nanofluids, which are base fluids with two or more nanoparticles, have altered physical and chemical properties that result in improved thermal conductivity [6]. However, adding these nanoparticles also alters the fluid's rheological properties [7], which are crucial parameters in designing efficient heat transfer systems. Hence, accurate prediction of these parameters is essential for optimising the performance of nanofluids in practical applications. Given this, classical prediction models have proved insufficient in elucidating nanofluid behaviour, leading to discrepancies between experimental findings and established models [8]. This limitation underscores the urgency for advanced modelling approaches capable of comprehending intricate nanoparticle–fluid interactions. Consequently, investigations are being done on diverse modelling techniques capable of yielding more precise forecasts for thermophysical properties of nanofluids, capturing their intricate nonlinear connections and complex nanoparticle–fluid interplays. In response to these challenges, numerous approaches [9–13] have been employed to model and predict the thermophysical properties of nanofluids.

Esfe et al. [14] applied the ANN technique to investigate the rheological properties of TiO_2 /water nanofluids, with temperature and volume fraction as predictors. The calculated R -squared value of 0.9998 indicated that the ANN model was able to accurately forecast nanofluid viscosity (μ_{nf}). Shahsavari et al. [15] used ANNs to forecast the thermal conductivity and μ_{nf} of liquid paraffin–alumina nanofluids based on experimental data and found that the ANN method provided accurate predictions. Afrand et al. [16] utilised the ANN modelling technique to estimate the rheological properties of Fe–EG nanofluid. They demonstrated that using the ANN method reduced the cost and time required for laboratory measurements. Mehrabi et al.

[17] formulated an ANFIS model to forecast the effective μ_{nf} . The outcomes generated by the suggested FCM-ANFIS model matched closely with the experimental measurements.

Colak et al. [18] investigated the μ_{nf} behaviour of ZrO₂/Water nanofluids prepared through a two-step method at varying concentrations (between 0.0125 and 0.2%) and temperatures. Experimental data revealed that μ_{nf} decreased with increasing temperature and increased with higher concentration. They developed both an ANN and a mathematical correlation to predict μ_{nf} . The ANN demonstrated high accuracy with an average error rate of -0.11% , while the mathematical model achieved an error rate of -0.74% . The study concluded that both the developed ANN and the mathematical correlation are effective tools for predicting μ_{nf} based on temperature and concentration variations.

Toghraie et al. [19] investigated the μ_{nf} of Ag/EG nanofluid over a temperature range of 25–55 °C and nanoparticle volume fraction of 0.2–2%. Using an Artificial Neural Network (ANN), they successfully predicted the μ_{nf} and compared the ANN's performance to a correlation method. The proposed algorithm identified the optimal ANN architecture, achieving accurate predictions based on input values of temperature and nanoparticle volume fraction. A comparison of the ANN and correlation results demonstrated the ANN's superior accuracy in predicting the μ_{nf} . The correlation method exhibited an MSE of 0.0012, SSE of 0.0512, and a maximum error of 0.0858. The study concluded that the ANN offers an effective means to predict Ag/EG μ_{nf} , reducing the need for costly experimental measurements.

In their study, Bhat et al. [20] explore μ_{nf} , investigating its interplay with nanoparticle concentration, size, and temperature. Employing CuO nanoparticles of varying sizes (15 nm, 45 nm, and 75 nm), the study observes μ_{nf} changes in the range of 1–4% volume concentrations and temperatures spanning 293 K to 353 K. The outcomes reveal notable trends: a 23% increase in effective μ_{nf} with added nanoparticles, an 80% decrease in μ_{nf} with temperature elevation, and a slight 0.5% increase in μ_{nf} as particle size grows. The research develops a correlation and employs ANN modelling for effective μ_{nf} prediction, showcasing the superior performance of ANN over the correlation. The R^2 values for the ANN and correlation models stand at 0.95 and 0.90, respectively.

In another study, Esfe et al. [21] focused on predicting the μ_{nf} of MWCNT-ZnO (50–50)/oil SAE50 nano-lubricant using an ANN. Their investigation incorporated three key factors: temperature, nanoparticle volume fraction (φ), and shear rate. They utilised principal component analysis (PCA) to detect outliers and conducted a sensitivity analysis to evaluate the significance of temperature and φ in influencing experimental variations in μ_{nf} . Remarkably, the developed ANN model, employing 7 neurons, exhibited a robust correlation between predicted and experimental data, effectively capturing the intricate behaviour of μ_{nf} in the nano-lubricant. This study's conclusion underscores the ANN's proficiency in accurately forecasting μ_{nf} and providing valuable insights into the complex interplay of temperature, φ , and the μ_{nf} characteristics of the MWCNT-ZnO (50–50)/oil SAE50 nano-lubricant system.

Esfe et al. [22] focused on predicting the μ_{nf} of a hybrid nano-lubricant MWCNT-Al₂O₃ (30:70)/Oil 5W50 using an ANN. The study investigated the influence of temperature and φ on shear rates (SR) and μ_{nf} prediction through ANN. The

feed-forward ANN employed a multilayer perceptron network (MLP) and effectively predicted μ_{nf} based on experimental temperature, SR, and φ data. Sensitivity analysis highlighted the importance of these factors in experimental μ_{nf} variations. The generated and tested ANN exhibited strong agreement between actual and predicted values. Comparison with other data processing methods, such as support vector machine (SVM), partial least squares (PLS), and principal component regression, showcased ANN's superior performance. The ANN model with 8 neurons also displayed small residual values for μ_{nf} , indicating its precision. Using the ANN BFGS algorithm, a low mean squared error (MSE) of $5.6e-02$ and a high % correlation coefficient of 97% were achieved for μ_{nf} prediction. Error diagrams underscored ANN's efficacy in determining μ_{nf} 's behaviour and the employed learning algorithm's effectiveness. Notably, the study also explored linear adjustments using the identity function in the output layer to adapt the trend of targets in some instances.

Yacine et al. [23] investigated the use of RSM and ANN methods to estimate the μ_{nf} of CuO-liquid paraffin nanofluids. The nanofluids were prepared at temperatures of 25–100 °C and mass fractions of 0.25–6 wt.%. The RSM method was used to develop a cubic polynomial model for the μ_{nf} . The model was observed to be accurate, with an R^2 value of 0.9230 and a maximum margin of deviation of 10.48%. The ANN model was more accurate than the RSM model, with an R^2 value of 0.9940 and a maximum margin of deviation of 3.27%.

Qing et al. [24] investigated the interplay of nanoparticle φ and temperature on dynamic μ_{nf} in Al₂O₃-MWCNT (40:60)—Oil SAE50 hybrid nano-lubricant. Their study involved 174 experiments encompassing various φ , temperatures, and shear rates. An ANN was developed using the trainbr/trainlm algorithm, exhibiting a high correlation coefficient of 0.999 and an MSE of 3.58 for predicting μ_{nf} . Comparative error diagrams and histograms validated the ANN's efficacy in assessing the efficiency of μ_{nf} and the training algorithms. The findings underscore that temperature notably influences μ_{nf} , while φ 's effect is more pronounced at lower temperatures. The shear rate also impacts μ_{nf} in a non-uniform manner.

This review shows that the rapid advancement of nanofluid rheology modelling, characterised by AI-based models and RSM applications, has led to accurate predictions of μ_{nf} under varying conditions. However, a significant research gap persists in the specific context of GNP-Alumina hybrid nanofluids, a relatively unexplored area within the field. This study aims to address this gap by advancing the predictive capabilities of these models in a novel and challenging nanofluid system. Also, while the existing literature review underscores successful applications of ANN and RSM techniques for predicting μ_{nf} , the unique characteristics of GNP-Alumina hybrid nanofluids introduce a new set of complexities. These complexities arise from the intricate interactions between mixing ratio and temperature, leading to nonlinear and non-uniform μ_{nf} changes. To address this challenge, our manuscript takes an innovative approach by optimising the AI-based models and RSM models to accurately forecast both μ_{nf} and μ_{rel} . This involves customising the models to capture the intricate interplay of mixing ratio and temperature, which has not been extensively explored in the existing literature.

Moreover, while ANNs have demonstrated their prowess in predicting nanofluid properties, including μ_{nf} , their architecture and performance optimisation

remain underexplored in the context of GNP-Alumina hybrid nanofluids. Our manuscript innovatively tackles this aspect, striving to develop ANN models that exhibit superior accuracy while considering the hybrid nature of the nanofluid. Additionally, incorporating μ_{rel} prediction, an aspect often overlooked in previous studies, adds further novelty to our work.

Thus, this study focuses on optimising AI models and RSM to predict the μ_{nf} and μ_{rel} of GNP-Alumina hybrid nanofluid. The study incorporates the influence of mixing ratio and temperature, which are known to have a significant impact on the properties of nanofluids. Two different AI models (ANN and ANFIS), RSM, and traditional linear regression (LR), were used to predict nanofluid properties. The AI models were optimised by varying the number and type of neurons and membership functions, respectively, while the RSM model was optimised by varying the source model. The performance of the models was evaluated using various measures of prediction accuracy, including margin-of-deviation (MOD), root mean square error (RMSE), mean absolute error (MAE), and mean absolute percentage error (MAPE).

It is essential to note that GNP and alumina were selected as the nanoparticles for the hybrid nanofluid due to their high surface area, good thermal conductivity, and relatively low cost. GNPs have a high surface area, meaning they can interact with many fluid molecules, leading to improved heat transfer [25]. GNP are also good heat conductors, which means they can quickly transfer heat from one part of the fluid to another. Alumina is also a good conductor of heat, which can help further improve the hybrid nanofluid's heat transfer performance [26]. Additionally, GNP and alumina are relatively inexpensive and easy to synthesise, making them a more practical choice than some other nanomaterials, such as carbon nanotubes.

The results of this study can be used to design efficient heat transfer systems using GNP-Alumina hybrid nanofluid. The optimised AI models and RSM provide accurate predictions of the μ_{nf} and μ_{rel} of the nanofluid, which can be used as input parameters for the design of heat transfer systems. This study focused on the μ_{nf} of the hybrid nanofluid based on several considerations rooted in both scientific and practical aspects. Firstly, the rheological behaviour of nanofluids plays a crucial role in various industrial applications, impacting their flow characteristics, stability, and overall performance. By accurately predicting μ_{nf} and μ_{rel} , this study aims to provide insights into the fluid's behaviour, which has implications for transportation, heat transfer, and mixing, among others. Secondly, the hybrid nature of GNP-Alumina nanofluids introduces complex interactions between the nanoparticles and base fluid, often leading to nonlinear and non-additive effects. By addressing the challenges of predicting these rheological properties, this study contributes to the fundamental understanding of nanofluid behaviour, which is essential for designing and optimising various technological applications.

Additionally, the study of rheological behaviour provides a foundation for further research into the thermophysical properties of nanofluids, including their thermal conductivity and convective heat transfer characteristics. These properties are closely interrelated with rheology and are critical factors in enhancing heat transfer efficiency.

2 Materials and methods

2.1 Experimental data collection

The research aims to evaluate the practicability of employing RSM and AI-based techniques, such as ANN and ANFIS, for modelling the influence of temperature and mixing ratio on the μ_{nf} of a hybrid nanofluid. To achieve this, the authors leveraged laboratory data sourced from Borode et al. [4]. This dataset was chosen due to its relevance and alignment with the objectives of our current research, as it provides a comprehensive set of experimental measurements specifically for GNP-Alumina hybrid nanofluids. Borode et al. [4] synthesised the hybrid nanofluid using a two-step approach and employing SDS surfactants to combine GNP with Al_2O_3 nanoparticles (20–30 nm diameter). The researchers used various mixing ratios of the hybrid nanoparticles (0.33, 1.00, and 3) to prepare the hybrid nanofluids at nanoparticle loading of 0.1 vol% while maintaining equal concentrations of surfactant (1:1). They observed all the nanofluid to be stable for over 48 h. The mixing ratio was calculated by dividing the weight of GNP by that of Al_2O_3 .

The researchers used a viscometer to measure the μ_{nf} of the resulting nanofluid samples at various temperatures (between 15 and 55 °C) and generated a dataset for future modelling processes. The dataset covers a range of mixing ratios (R) and temperatures (T), enabling us to incorporate the effects of these factors on μ_{nf} and μ_{rel} predictions, which is a central aspect of our investigation.

2.2 Artificial neural network (ANN) modelling

An ANN was developed using MATLAB software to model the μ_{nf} and μ_{rel} of the hybrid nanofluid. The MATLAB 2020a software platform facilitated the construction and training of the neural network architectures, allowing for the iterative adjustment of parameters to achieve the highest predictive accuracy. The ANN architecture was optimised through adjustment of the number of neurons and trained with 70% of the experimental data, while 15% was used for testing and the remaining 15% for validation. To evaluate the accuracy of the ANN model, the forecasted values were compared with the laboratory data, and the mean square error (MSE) was calculated as a measure of efficacy. Equation (4) presents the formula used to calculate the MSE [27], which indicates the disparity between the observed data and the projected values derived from the ANN predictions.

$$\text{MSE} = \frac{1}{n} \sum_{i=1}^n (\text{Actual Value}_i - \text{Predicted value}_i)^2 \quad (1)$$

where n is the datapoint number.

Artificial neural networks (ANNs) are a type of machine learning algorithm that takes inspiration from the structure and function of the human brain [28].

They are made up of interconnected artificial neurons that process and analyse data. Each neuron receives input signals from its neighbouring neurons, applies an activation function to process the information, and passes the output to other neurons in the network. ANNs learn by modifying the strengths of the connections between neurons to enhance the network's capability to provide precise predictions or classifications. Neurons are modelled as mathematical functions that take input values (x_j), multiply them by corresponding weights (w_{ij}), add a bias term (b_i), and then apply an activation function (f) to produce an output μ_i . The mathematical model of a neuron is shown in Eq. (5) [29]. To assess the accuracy of the ANN model in predicting μ_{nf} , we calculated the mean square error (MSE) using the actual and predicted values of μ_{nf} , where n is the number of data points.

$$\mu_i = f\left(\sum_{j=1}^n (w_{ij}x_j + b_i)\right) \quad (2)$$

To develop an efficient ANN, one must consider factors such as the learning algorithm, number of neurons, and choice of activation function. The Levenberg–Marquardt algorithm was selected as the learning algorithm for this study. This algorithm uses an iterative approach to minimise the disparity between predicted and actual output [30]. In addition, this algorithm enables the network to progressively enhance its predictive accuracy. It is important to note that the efficiency of the ANN is influenced by its architecture, including the number of neurons and the selection of activation functions. A two-layer feed-forward network was employed in this study. The hidden layer used the tansig activation function, while the output layer employed the purelin activation function. These functions, represented by Eqs. (6) and (7), respectively [31], contribute to processing input data and producing accurate predictions.

$$\text{tansig}(n) = \frac{2}{1 + e^{-2n}} - 1 \quad (3)$$

$$f(x) = \frac{1}{1 + \exp(-x)} \quad (4)$$

Numerous neuron numbers, spanning from 1 to 15, were examined for network optimisation, and the most effective count was chosen. Given the random nature of weight and bias generation in the network, multiple runs were conducted for each neuron number, and the average performance was employed as the metric. The optimal neuron number was identified through iterative adjustments, varying the neuron number and assessing the resulting network output.

2.3 Adaptive neuro-fuzzy inference system

ANFIS is an effective hybrid method for modelling various systems by combining fuzzy techniques and ANN [32]. The shortcomings of each approach can be reduced

by the other, which ultimately enhances the efficiency of the system, known as neuro-fuzzy.

The ANFIS modelling based on grid partitioning (GP) Sugeno-based fuzzy inference systems was performed using MATLAB R2020a software with the Fuzzy Logic Toolbox. The ANFIS models were meticulously crafted and fine-tuned within the MATLAB environment, leveraging its computational power and flexibility to effectively handle the intricate relationships between variables. The GP-ANFIS method is efficient for small sets of input variables, and it employs membership functions (MFs) to partition input data into rectangular subspaces, which form the basis for fuzzy regions [33, 34]. The number of membership functions (MFs) can vary depending on the significance and impact of the input variables. While more fuzzy rules can lead to better performance, they also increase computational demands and model complexity. There is a limit to the number of fuzzy rules that can be effectively used, as too many rules can lead to the “curse of dimensionality” [35]. In GP-ANFIS, the number of MFs allocated to each input is limited to a predetermined range based on the available data points. This ensures that the model remains manageable and avoids having too many rules for the available data.

In this study, the ANFIS model was trained using 85% of the experimental data, and the remaining 15% of the data was used for testing the model. The ANFIS model was used to predict the μ_{nf} and μ_{rel} of the hybrid nanofluids based on the mixing ratio and temperature inputs. The number and type of membership functions (MF) for each input variable were optimised to achieve the best performance of the ANFIS model. Various MF types were considered in fuzzy logic systems, and the number of MF was varied from 3 to 4 for the mixing ratio and 4–5 for the temperature. The MF types evaluated include Triangular (TriMF), Trapezoidal (TrapMF), Generalized Bell (GbellMF), Gaussian (GaussMF), Double Gaussian (Gauss2MF), Pi-shaped (PiMF), Difference of Sigmas (DsigMF), and Product of Sigmas (PsigMF) Membership Functions. The performance of the ANFIS model was evaluated using the MSE between the predicted and actual values of μ_{nf} and μ_{rel} . The best ANFIS model was selected based on the minimum MSE value.

2.4 Response surface methodology (RSM) modelling

The statistical method of RSM was utilised to model the μ_{nf} by fitting a response surface to laboratory data through the Design of Experiments (DoE). Subsequently, regression analysis was applied to establish a response surface model based on the collected data. The RSM models were expertly constructed using the Design Expert 13 software. This software facilitated the fitting of response surfaces to experimental data, enabling the exploration of various source models and their optimisation to accurately capture the complex interactions between input factors and μ_{nf} responses. The input parameters and output were employed to suggest a variety of polynomial functions resembling first-, second-, or third-order equations as presented in Eqs. (5, 6 and 7) [23, 36, 37]. The selection of the most suitable polynomial function, which closely matches the data was chosen by the user based on mathematical criteria. The Design Expert software determined the quadratic equation’s coefficients through

multiple regression analysis of the experimental results. The regression equation’s strength was estimated using R^2 and R . Graphical techniques were employed to visualise the model’s ability to fit the actual data, and ANOVA was utilised to assess the model’s significance. The RSM analysis code and factors definition are presented in Table 1.

$$\mu = \alpha_0 + \alpha_1 T + \alpha_2 R \tag{5}$$

$$\mu = \beta_0 + \beta_1 T + \beta_2 R + \beta_3 RT + \beta_4 T^2 + \beta_5 R^2 \tag{6}$$

$$\mu = \gamma_0 + \gamma_1 T + \gamma_2 R + \gamma_3 RT + \gamma_4 T^2 + \gamma_5 R^2 + \gamma_6 T^2 R + \gamma_7 TR^2 + \gamma_8 T^3 + \gamma_9 R^3 \tag{7}$$

In the application of RSM to predict the μ properties of GNP-alumina hybrid nanofluids, the selection of optimal source models played a pivotal role in achieving precise predictions. The study explored various source models to effectively capture the intricate relationships between input factors (mixing ratio and temperature) and viscosity responses (μ_{nf} and μ_{rel}). The options considered for viscosity predictions encompassed Linear, Two-Factor Interaction (2FI), Quadratic, Cubic, and Quartic models, each offering increasing complexity to represent nonlinearities. Similarly, for μ_{rel} predictions, the same models were evaluated. These source models were meticulously optimised to minimise prediction errors and closely align with experimental data. By systematically comparing their performance, the study identified the most suitable source models that accurately portrayed the interplay between mixing ratio, temperature, and μ properties of GNP-alumina hybrid nanofluids. This rigorous approach ensured the chosen source models precisely captured the μ responses and facilitated reliable predictions under varying experimental conditions.

2.5 Comparative analysis

The study compared the performance of ANFIS, ANN and RSM models with linear regression analysis. Evaluation metrics such as R^2 , and error metrics were used to assess the performance of the different models. The error metrics include the margin of deviation (MOD), mean absolute percentage error (MAPE), mean absolute error (MAE), residual sum of squares (RSS), and root mean square error (RMSE). The error metrics were calculated using Eqs. (8, 9, 10, 11, 12) to evaluate the models’ performance [38, 39].

Table 1 Code and factors for the RSM architecture

Factor	Name	Minimum	Maximum	Coded low (-1)	Coded high (+1)
A	Mixing ratio	0	3	0	3
B	Temperature (°C)	15	55	15	55

$$\text{MOD} = \frac{\text{actual value} - \text{predicted value}}{\text{actual value}} \times 100 \tag{8}$$

$$\text{MAPE} = \frac{1}{n} \sum_{i=1}^n |\text{MOD}_i| \tag{9}$$

$$\text{MAE} = \frac{1}{n} \sum_{i=1}^n |\text{actual value}_i - \text{Predicted value}_i| \tag{10}$$

$$\text{RSS} = \sum_{i=1}^n (\text{Actual value}_i - \text{Predicted value}_i)^2 \tag{11}$$

$$\text{RSME} = \sqrt{\frac{\text{RSS}}{n}} \tag{12}$$

Table 2 The correlation coefficient and sorted MSE performance of the ANN viscosity output at different neuron number

Number of neuron	Coefficient of correlation				MSE performance			
	Train	Validation	Testing	All	Train	Validation	Testing	All
4	1.0000	1.0000	0.9998	0.9998	3.58E-06	2.47E-05	4.69E-05	1.33E-05
7	0.9997	1.0000	0.9998	0.9996	3.73E-05	1.72E-05	4.49E-05	3.55E-05
3	0.9997	0.9998	1.0000	0.9993	2.74E-05	6.23E-05	1.77E-04	5.51E-05
6	0.9998	1.0000	0.9976	0.9993	1.74E-05	8.35E-05	2.33E-04	5.96E-05
2	0.9979	0.9999	0.9951	0.9993	7.60E-05	1.75E-05	3.62E-05	6.13E-05
10	0.9997	0.9983	0.9973	0.9989	3.57E-05	3.20E-04	3.17E-04	1.21E-04
1	0.9990	0.9999	0.9989	0.9985	8.03E-05	3.90E-04	1.47E-04	1.37E-04
5	0.9998	0.9658	0.9979	0.9983	1.86E-05	7.67E-04	1.88E-04	1.56E-04
11	1.0000	0.9979	0.9941	0.9958	1.95E-07	3.22E-04	2.16E-03	3.73E-04
15	1.0000	0.9625	0.9846	0.9951	1.51E-07	5.42E-04	2.18E-03	4.09E-04
14	0.9994	0.9976	0.9988	0.9952	5.86E-05	5.70E-04	1.99E-03	4.25E-04
9	0.9995	0.9930	0.9999	0.9912	2.93E-05	1.77E-03	3.33E-03	7.86E-04
8	1.0000	0.9801	0.9785	0.9882	3.11E-06	3.81E-03	4.42E-03	1.24E-03
13	0.9968	0.9805	0.9324	0.9873	4.57E-04	4.86E-03	2.48E-03	1.42E-03
16	0.9791	0.9863	0.9898	0.9766	2.01E-03	1.47E-03	2.73E-03	2.03E-03
12	0.9999	0.9867	0.9457	0.9721	1.26E-05	1.09E-03	1.86E-02	2.96E-03

Table 3 The correlation coefficient and sorted MSE performance of the ANN relative viscosity output at different neuron number

Number of neuron	Coefficient of correlation				MSE performance			
	Train	Validation	Testing	All	Train	Validation	Testing	All
5	0.9991	0.9967	0.9994	0.9908	2.34E-06	8.26E-05	6.68E-05	2.40E-05
11	0.9939	0.9993	0.8516	0.9805	9.90E-06	2.40E-06	2.20E-04	4.03E-05
14	0.9664	0.9991	0.9970	0.9789	5.02E-05	1.77E-05	2.73E-05	4.19E-05
12	0.9758	0.9730	0.9384	0.9673	4.28E-05	7.96E-05	1.66E-04	6.68E-05
6	0.9988	0.9976	0.9000	0.9668	2.82E-06	2.54E-05	4.58E-04	7.44E-05
15	0.9553	0.9996	0.9993	0.9654	5.54E-05	1.70E-04	1.34E-04	8.44E-05
9	0.9736	0.9902	0.9807	0.9596	5.22E-05	2.46E-04	1.14E-04	9.05E-05
10	0.9996	0.8754	0.9481	0.9479	9.82E-07	4.04E-04	2.53E-04	9.92E-05
13	0.9635	0.9541	0.9870	0.9478	6.50E-05	8.93E-05	3.05E-04	1.05E-04
16	0.9961	0.9997	0.8760	0.9522	1.45E-05	3.19E-04	3.30E-04	1.08E-04
2	0.9282	0.9538	0.9961	0.9389	9.03E-05	1.80E-04	1.85E-04	1.18E-04
4	0.9784	0.9991	0.9009	0.9465	4.02E-05	6.10E-06	6.13E-04	1.21E-04
8	0.9598	0.9614	0.9986	0.9411	7.35E-05	4.15E-04	1.25E-04	1.32E-04
7	0.9481	0.9975	0.9537	0.9131	1.01E-04	1.66E-04	4.57E-04	1.64E-04
3	0.9393	0.9505	0.8738	0.9151	1.77E-04	1.07E-04	2.75E-04	1.81E-04
1	0.8894	0.9290	0.9779	0.8902	2.46E-04	1.61E-04	5.14E-05	2.04E-04

3 Results and discussion

3.1 Artificial neural network

Tables 2 and 3 present the efficacy of ANN in predicting the μ_{nf} and μ_{rel} , respectively, of GNP-alumina hybrid nanofluid at various neuron numbers. The ANN model was trained, validated, and tested by utilising a set of input variables and their corresponding μ_{nf} and μ_{rel} values. Three metrics were used to evaluate the ANN: correlation coefficient (R) and MSE for training, validation, testing and overall. The model's effectiveness was measured by analysing the MSE values for each set of neurons. A lower MSE value indicates that the model has better predictive performance. The results indicate that the ANN model with 4 neurons achieved the best performance in terms of both R and MSE for all the μ_{nf} data sets, while the ANN model with 5 neurons achieved the best performance in terms of both R and MSE for all the μ_{rel} data sets. The ANN schematics for the optimal neuron number are presented in Fig. 1a, b. The figure indicates that the ANN model has three layers: input, hidden, and output. The input layer receives the input parameters, the hidden layer performs the learning based on the number of neurons, and the output layer produces the prediction values.

Figures 2 and 3 depict the relationship between the ANN output data point and the actual data point for the training, validation, testing, and overall data sets using the optimal number of neurons for μ_{nf} and μ_{rel} , respectively. In the training data set shown in the figures, the R -value is 1 and 0.9991 for μ_{nf} and μ_{rel} , respectively. The

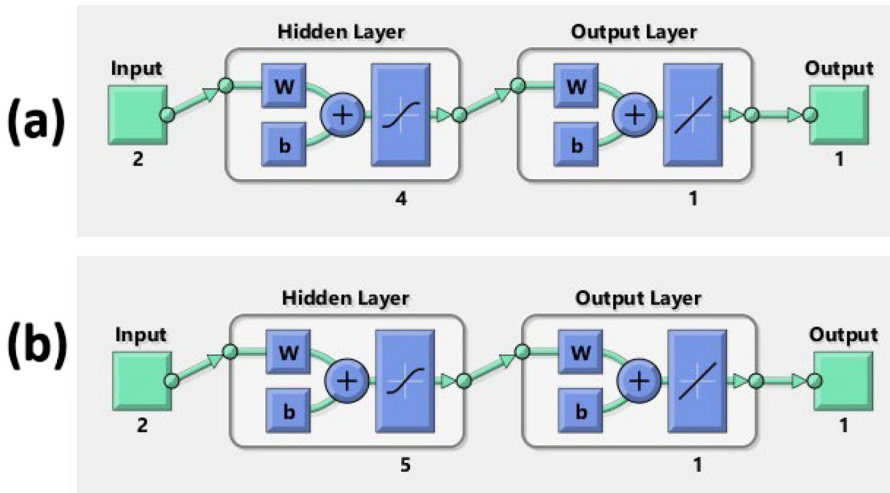


Fig. 1 ANN schematics of (a) viscosity and (b) relative viscosity for optimum neuron number

validation and testing data sets for the μ_{nf} have an R -value of 0.98788 and 0.9999, respectively. Conversely, the R for the μ_{rel} in the validation and testing datasets are 0.99671 and 0.99936, respectively. Overall, the figures indicated a strong correlation between the forecasted and observed values for μ_{nf} and μ_{rel} . However, it is worth noting that the ANN model for μ_{nf} is more suitable for its dataset than the ANN model for μ_{rel} (Fig. 4). Therefore, the ANN model for μ_{nf} is expected to have higher accuracy and dependability in forecasting future observations than the ANN model for μ_{rel} .

3.2 Adaptive neuro-fuzzy inference system

Tables 4 and 5 show the optimisation results of the membership function (MF) type and number of MFs for the input parameters of μ_{nf} and μ_{rel} , respectively. The table presents the MSE values obtained for different combinations of the number of MFs and the MF types. The rows represent the different types of MF evaluated, while the columns represent the different combinations of numbers of MF used for the mixing ratio (R) and temperature (T) inputs. For example, (3 4) means 3 MF for mixing ratio and 4 MF for temperature. This optimisation aims to identify the best combination of MF type and number of MFs that leads to the smallest MSE value. In this case, the smallest MSE value for the μ_{nf} is achieved for both DsigMF and PsigMF with three and five MFs for the input parameters (R and T), respectively, as shown by the value of 2.86E-06, highlighted (bold) in Table 4.

Conversely, the lowest MSE value for the μ_{rel} is achieved for GbellMF with four and five MFs for the input parameters (R and T), respectively, as shown by the value of 1.29E-05, highlighted (bold) in Table 5. The lowest MSE value indicates the best performance of the ANFIS model, which can be used to predict the μ_{nf} and μ_{rel} of

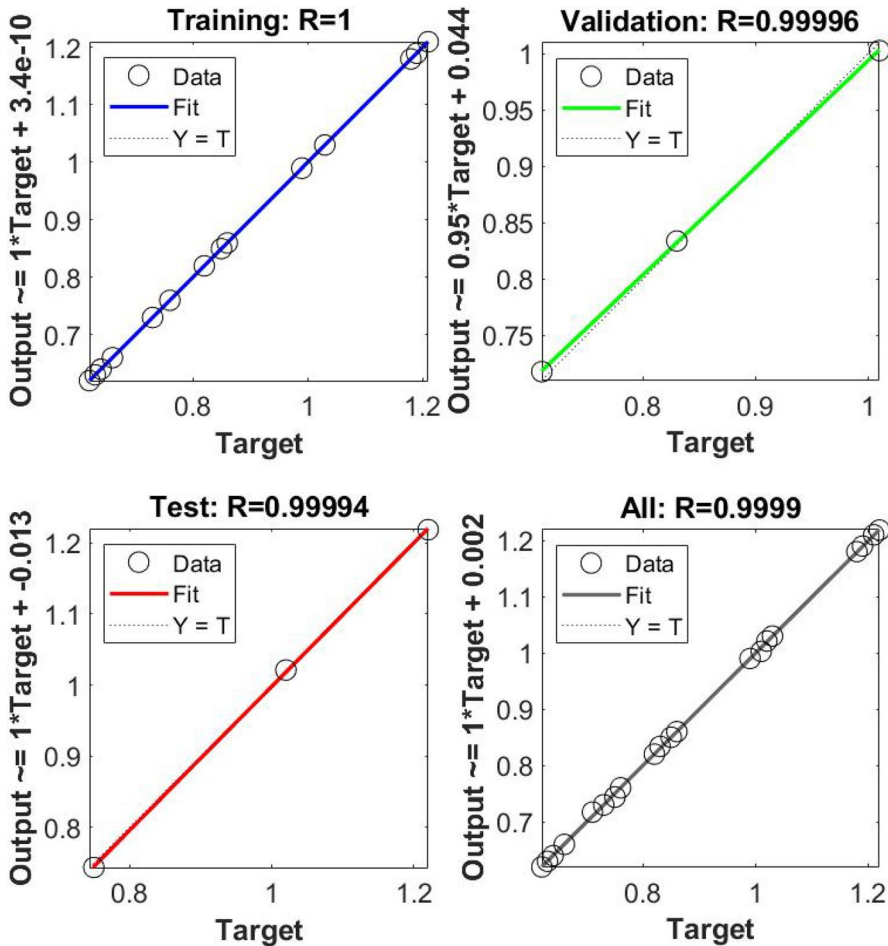


Fig. 2 ANN training, validation, testing and overall viscosity data outputs

hybrid nanofluids based on the mixing ratio and temperature inputs. The corresponding structures for the optimal MF parameters of the outputs are illustrated in Fig. 5.

To support the result of this optimisation, a graph, which depicts the linear fitting of the predicted value generated using the optimal ANFIS Model for both μ_{nf} and μ_{rel} is presented in Fig. 6a, b. This graph enables the visualisation of the accuracy of the model's prediction and estimation of its correlation parameters. In this study, the graphs showed a high correlation between the predicted and actual values for both μ_{nf} and μ_{rel} . The R^2 values were 0.9999 and 0.9872, respectively, indicating a strong correlation between the predicted and actual values. The slope of the fitted line was close to 1, indicating that the ANFIS model accurately predicted the μ_{nf} and μ_{rel} of the hybrid nanofluids. This result indicates that the ANFIS model of the μ_{nf} fits its data better than that of μ_{rel} . This shows that

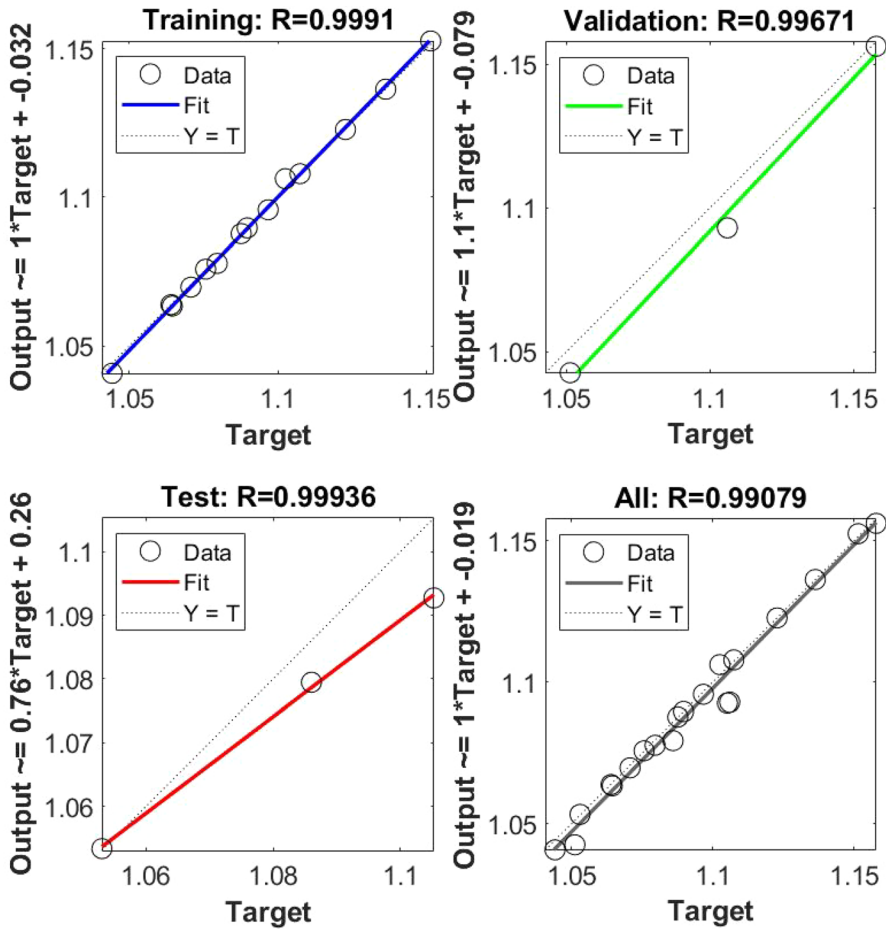


Fig. 3 ANN training, validation, testing and overall relative viscosity data outputs

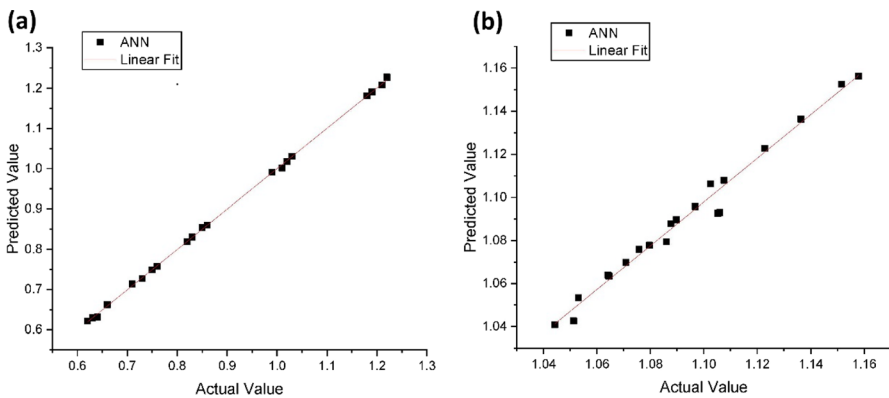


Fig. 4 Linear fitting of ANN predicted value in relation to the experimental data of (a) viscosity and (b) relative viscosity

Table 4 Optimisation of the MF type and the number of MF for the input parameters of the viscosity

MF type	Number of MFs ($R T$)				
	(3 3)	(3 4)	(3 5)	(4 4)	(4 5)
TriMF	1.13E-05	1.01E-05	2.44E-05	1.07E-04	4.25E-06
TrapMF	3.69E-05	3.20E-05	2.82E-02	4.01E-06	2.99E-06
GbellMF	1.26E-05	4.85E-06	2.88E-06	2.99E-04	5.69E-06
GaussMF	1.30E-05	1.15E-04	2.89E-06	1.51E-04	4.82E-06
Gauss2MF	1.28E-05	4.12E-06	2.96E-06	9.92E-06	3.28E-06
PiMF	3.71E-05	3.23E-05	2.82E-02	4.14E-06	2.97E-06
DsigMF	1.33E-05	4.04E-06	2.86E-06	1.17E-05	1.56E-05
PsigMF	1.33E-05	4.04E-06	2.86E-06	1.17E-05	1.55E-05

Table 5 Optimisation of the MF type and the number of MF for the input parameters of the relative viscosity

MF type	Number of MFs ($R T$)				
	(3 3)	(3 4)	(3 5)	(4 4)	(4 5)
TriMF	1.15E-04	2.44E-05	5.63E-05	3.15E-02	1.74E-05
TrapMF	8.11E-05	7.39E-05	6.02E-02	2.44E-05	1.52E-05
GbellMF	3.38E-05	2.48E-05	1.48E-05	4.14E-02	1.29E-05
GaussMF	3.42E-05	2.45E-05	1.49E-05	3.78E-02	1.97E-05
Gauss2MF	3.36E-05	2.45E-05	1.51E-05	4.47E-02	1.47E-05
PiMF	8.10E-05	7.39E-05	6.02E-02	2.44E-05	1.52E-05
DsigMF	3.36E-05	2.47E-05	1.48E-05	4.12E-02	1.46E-05
PsigMF	3.36E-05	2.47E-05	1.48E-05	4.12E-02	1.46E-05

the ANFIS model of μ_{nf} is likely more accurate and reliable in predicting future observations than that of μ_{rel} .

3.3 Response surface methodology

The RSM is a statistical technique used to determine the optimal combination of input variables to produce the best possible output. Table 6 presents the RSM analysis results for the outputs (μ_{nf} and μ_{rel}). The table shows the different model types (linear, 2-factor interaction (2FI), quadratic, cubic, and quartic) tested for each output and their corresponding Sequential p -value, Adjusted R^2 , and Predicted R^2 . The Sequential p -value indicates the significance of each model, with smaller p -values less than 0.05 indicating more significant models. The Adjusted R^2 evaluates the extent to which the model conforms to the data while considering the number of variables included in the model. The Predicted R^2 evaluates the accuracy of the model's predictions for new data.

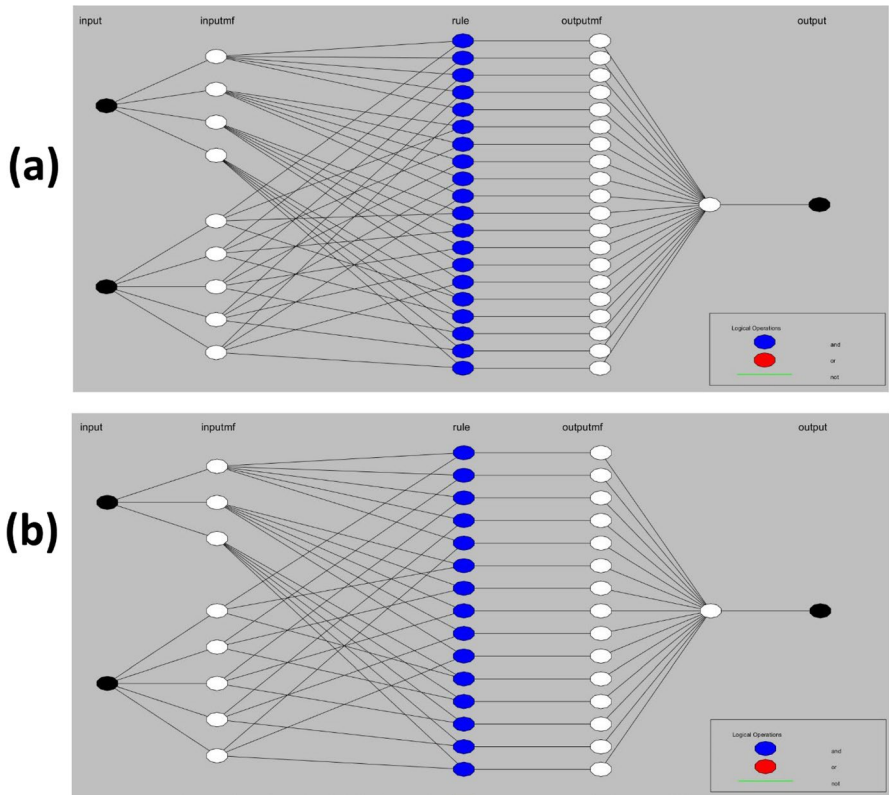


Fig. 5 Optimum ANFIS structure for the modelling of (a) viscosity and (b) relative viscosity

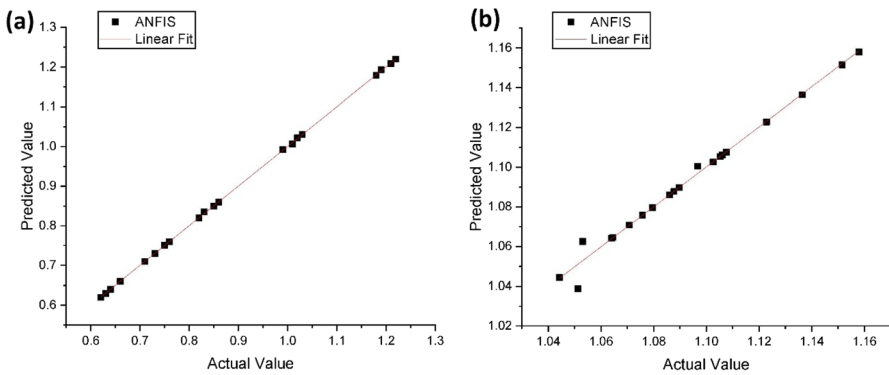


Fig. 6 Linear fitting of ANFIS predicted value in relation to the experimental data of (a) viscosity and (b) relative viscosity

Table 6 Optimal selection of the best RSM model

Output	Source	Sequential p -value	Adjusted R^2	Predicted R^2	
Viscosity	Linear	<0.0001	0.9736	0.9666	
	2FI	0.9383	0.9719	0.9579	
	Quadratic	<0.0001	0.9982	0.9977	Suggested
	Cubic	0.92	0.9976	0.9961	
	Quartic	0.0029	0.9996	0.9967	Aliased
Relative viscosity	Linear	<0.0001	0.7617	0.7173	
	2FI	0.1373	0.7804	0.7493	
	Quadratic	0.0393	0.8419	0.8046	Suggested
	Cubic	0.9955	0.7826	0.6425	
	Quartic	0.0021	0.9701	0.671	Aliased

For the μ_{nf} output, the quadratic model is suggested as the optimal model because it has a Sequential p -value of less than 0.0001 and the highest Adjusted R^2 and Predicted R^2 values among all the models tested. For the μ_{rel} output, the quadratic model is also suggested as the optimal model because it has a Sequential p -value of 0.0393 and the highest Adjusted R^2 and Predicted R^2 values among all the models tested, except for the Quartic model. However, the Quartic model has a low Sequential p -value of 0.0021, which suggests it is significant. Still, it is aliased, meaning it cannot be estimated uniquely from the data. Therefore, the quadratic model is the recommended model for the μ_{rel} output.

Table 7 ANOVA findings for the recommended model

	Source	Sum of squares	df	Mean square	F -value	p -value	
Viscosity	Model	0.8062	5	0.1612	2054.83	<0.0001	Significant
	A-mixing ratio	0.0048	1	0.0048	61.7	<0.0001	
	B-temperature	0.6934	1	0.6934	8836.41	<0.0001	
	AB	7.39E-06	1	7.39E-06	0.0941	0.7635	
	A ²	0.0008	1	0.0008	10.62	0.0057	
	B ²	0.0171	1	0.0171	218.56	<0.0001	
	Residual	0.0011	14	0.0001			
	Cor total	0.8073	19				
Relative viscosity	Model	0.0172	5	0.0034	21.24	<0.0001	Significant
	A-mixing ratio	0.0083	1	0.0083	51.41	<0.0001	
	B-temperature	0.0085	1	0.0085	52.6	<0.0001	
	AB	0.0006	1	0.0006	3.4	0.0864	
	A ²	0.0013	1	0.0013	8.23	0.0124	
	B ²	1.67E-07	1	1.67E-07	0.001	0.9748	
	Residual	0.0023	14	0.0002			
	Cor total	0.0195	19				

Table 7 shows the results of an ANOVA (Analysis of Variance) for the recommended model for two outputs: μ_{nf} and μ_{rel} . ANOVA is a statistical technique utilised for examining the variation among different groups or factors in a dataset. The table shows the sources of variation in the data, including the Model, A-Mixing Ratio, B-Temperature, AB interaction, A^2 , B^2 , Residual, and Cor Total. For each source of variation, the table provides the Sum of Squares, degrees of freedom (df), Mean Square, F-value, and p -value. The F -value is the ratio of the variance explained by the model to the variance not explained by the model. For both the μ_{nf} and the μ_{rel} output, the ANOVA table shows that the model is significant (p -value < 0.0001), indicating that the recommended model is a good fit for the data. Among the variables in the model, A, B, A^2 , and B^2 are also significant (p -values < 0.05). At the same time, AB interaction is insignificant (p -value > 0.05) for the μ_{nf} output and weakens the μ_{rel} output.

Table 8 shows the coefficient estimates for the factors in coded units for the response variables of μ_{nf} and μ_{rel} . For μ_{nf} and μ_{rel} , the intercept is correspondingly 1.12 and 0.8685, indicating the expected value of the response when both factors are at their midpoint. For both outputs, the coefficient estimates for A is 0.0269 and 0.0205, respectively, indicating that increasing A levels positively affect μ_{nf} and μ_{rel} . The coefficient estimate for B is 0.031 and -0.2797 correspondingly for both outputs, indicating that increasing B levels positively affect the μ_{nf} . At the same time, it exhibits a negative effect on μ_{rel} . The AB coefficient estimate for μ_{nf} is 0.0096, indicating that the interaction effect is positive but relatively small, while that of μ_{rel} is close to zero (0.0011), indicating little evidence of an interaction effect. The A^2 coefficient estimate for both outputs is negative, indicating a curvature in the effect of A on μ_{nf} and μ_{rel} . Conversely, the B^2 coefficient estimate of the μ_{nf} is close to zero, indicating little evidence of a quadratic effect of B. At the same time, that of μ_{rel} is positive (0.07), indicating that there is evidence of a quadratic effect of B on μ_{rel} .

Table 8 Coefficient estimate in terms of the coded factors

	Factor	Coefficient estimate	df	Standard error	95% CI low	95% CI high	VIF
Viscosity	Intercept	1.12	1	0.0072	1.1	1.13	
	A	0.0269	1	0.0038	0.0189	0.035	1.05
	B	0.031	1	0.0043	0.0218	0.0402	1.13
	AB	0.0096	1	0.0052	-0.0016	0.0207	1.13
	A^2	-0.0229	1	0.008	-0.04	-0.0058	1.05
	B^2	0.0002	1	0.0068	-0.0144	0.0148	1
Relative viscosity	Intercept	0.8685	1	0.005	0.8577	0.8793	
	A	0.0205	1	0.0026	0.0149	0.0262	1.05
	B	-0.2797	1	0.003	-0.2861	-0.2733	1.13
	AB	0.0011	1	0.0036	-0.0066	0.0089	1.13
	A^2	-0.0181	1	0.0056	-0.03	-0.0062	1.05
	B^2	0.07	1	0.0047	0.0598	0.0802	1

Additionally, the VIF (variance inflation factor) is provided for each factor, which measures how much the variance of a coefficient estimate is inflated due to collinearity with other factors. The VIF for each factor indicates the extent to which that factor is linearly related to the other factors in the model. A VIF of 1 indicates no multicollinearity, while VIFs greater than 1 indicate increasing levels of multicollinearity. Generally, VIFs less than 10 are considered tolerable, but the threshold may depend on the specific context. As presented in Table 8, all the VIFs are less than or equal to 1.13, indicating no significant multicollinearity present in the model. Therefore, we can conclude that the model is not affected by multicollinearity, and the estimates for the coefficients are reliable.

The model-coded equation for the μ_{nf} and μ_{rel} are presented in Eq. (13 and 14), respectively. The coded equation can predict the response for given levels of the factors in a way that is independent of the actual units used to measure the factors. This is because the coded levels are standardised to a range of -1 to $+1$, corresponding to the low and high levels of the factors. The relative impact of each factor on the response can be determined by comparing the magnitude and direction of the coefficients. For example, in Table 8, it can be observed that the coefficient for factor B is larger than the coefficient for factor A in both the μ_{nf} and μ_{rel} equations, suggesting that factor B has a stronger effect on the response than factor A. The equation expressed in terms of the actual factors for both outputs are presented in Eqs. (15 and 16). These equations can predict the response for a given level of each factor.

$$\mu_{nf} = 0.8685 + 0.0205A - 0.2797B + 0.0011AB - 0.0181A^2 + 0.0700B^2 \tag{13}$$

$$\frac{\mu_{nf}}{\mu_{water}} = 1.12 + 0.0269A + 0.0310B + 0.0096AB - 0.0229A^2 + 0.0002B^2 \tag{14}$$

$$\mu_{nf} = 1.53562 + 0.036539R - 0.026290T + 0.000037RT - 0.008044R^2 + 0.000175T^2 \tag{15}$$

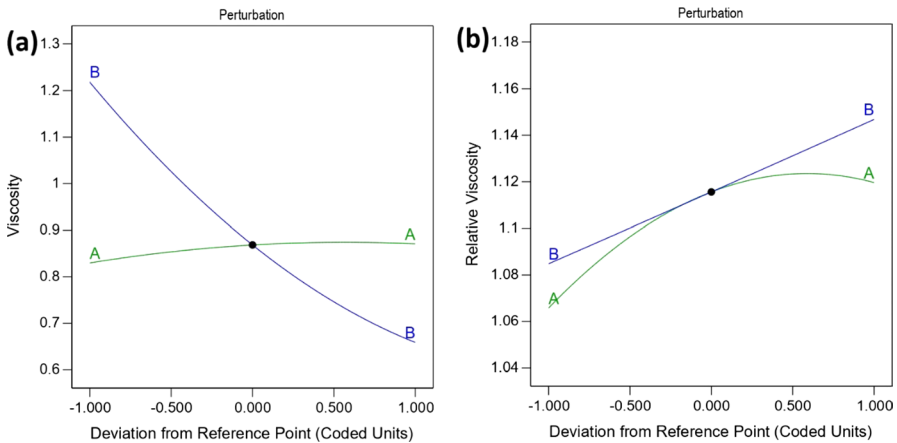


Fig. 7 Perturbation plot for the RSM modelling of (a) viscosity and (b) relative viscosity

$$\frac{\mu_{nf}}{\mu_{water}} = 1.02895 + 0.037309R + 0.001033T + 0.000319RT - 0.010169R^2 + 5.46429E - 07T^2 \tag{16}$$

The influence of two factors on the μ_{nf} and μ_{rel} behaviour is showcased in Fig. 7a, b using perturbation plots. These visualisations offer insights into the correlation between factors and the system’s outcome. The creation of the plot involves modifying one factor while keeping the other parameters constant and noting the resultant alterations in the response. By doing this, the curvature of the response surface can be visualised, and any interactions between the factors can be identified. The response sensitivity to a particular factor is reflected in the slope of its line, while the line’s curvature indicates a relationship with other variables. From the result, it can be inferred that factor B exerts the most substantial impact on both μ_{nf} and μ_{rel} , while factor A has the least.

Figure 8a, b displays contour plots illustrating the effect of mixing ratio and temperature on the μ_{nf} and μ_{rel} . In Fig. 8a, the contour plot for μ_{nf} shows that as the mixing ratio increases, the μ_{nf} of the nanofluid also increases. This indicates that a higher concentration of the GNP in the hybrid nanoparticle mixture leads to a thicker or more viscous hybrid nanofluid. Additionally, as the temperature decreases, the μ_{nf} of the nanofluid also increases. This indicates that the fluid becomes more viscous at lower temperatures, which can have implications for its flow properties and behaviour. Many published studies [40–43] support this observation.

In Fig. 8b, the contour plot for μ_{rel} shows that as the mixing ratio increases, the μ_{rel} of the fluid also increases. This indicates that a higher concentration of the GNP in the hybrid nanoparticle mixture leads to a greater increase in μ_{nf} compared to a base fluid. This behaviour can be attributed to various mechanisms through which nanoparticles interact with the base fluid, influencing μ properties. Notably, these

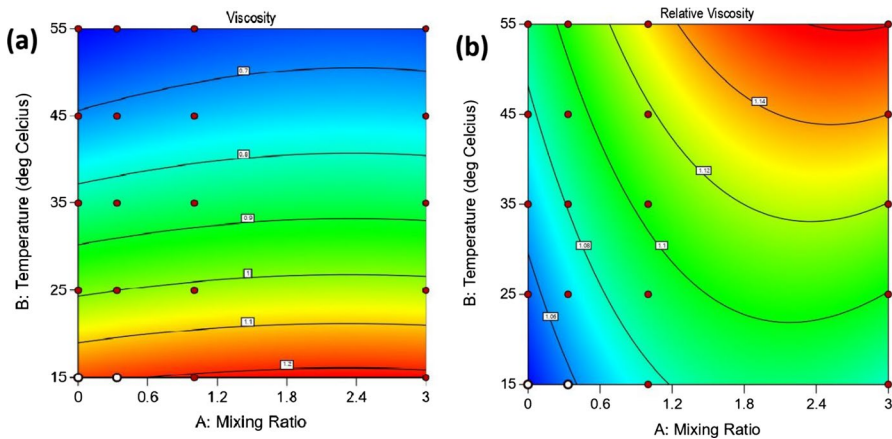


Fig. 8 Contour of RSM predicted values of (a) viscosity and (b) relative viscosity in relation to the input parameters

mechanisms encompass physical adsorption and chemical bonding phenomena. Physical adsorption, where nanoparticles adhere to the base fluid molecules' surface, can contribute to μ increase by forming a nanoparticle layer around the molecules. Conversely, chemical bonding, involving nanoparticles bonding with base fluid molecules, can further elevate μ by establishing a network of nanoparticles within the base fluid.

Additionally, as the temperature decreases, the μ_{rel} of the fluid also increases. This indicates that at lower temperatures, the fluid becomes more resistant to flow than the base fluid, which can also affect its behaviour and performance. This temperature-dependent behaviour is rooted in the amplified kinetic energy or Brownian motion of base fluid molecules at higher temperatures, facilitating smoother movement and reducing resistance. Consequently, the enhanced fluidity results in decreased μ . Many previous studies [41, 44–46] have also made a similar observation, emphasising the significance of temperature and nanoparticle concentration in influencing the μ behaviour of the hybrid nanofluid.

The predicted values generated using the RSM model for μ_{nf} and μ_{rel} were compared with experimental data through linear fitting. The results of this analysis are presented in Fig. 9a, b, which shows the linear fitting lines for the predicted and experimental values for both μ_{nf} and μ_{rel} . The high R^2 values obtained for both variables (0.9986 for μ_{nf} and 0.8835 for μ_{rel}) indicate a strong correlation between the predicted and experimental values. These findings highlight the effectiveness of RSM in predicting μ_{nf} and μ_{rel} and provide valuable insight into the relationships between these variables.

3.4 Comparison of the modelling techniques

In this study, the μ_{nf} and μ_{rel} were predicted using three different modelling techniques: ANN, ANFIS and RSM. All these techniques are commonly used in engineering and statistical modelling, and each has its strengths and limitations. To comprehensively compare these techniques and the traditional linear regression (LR)

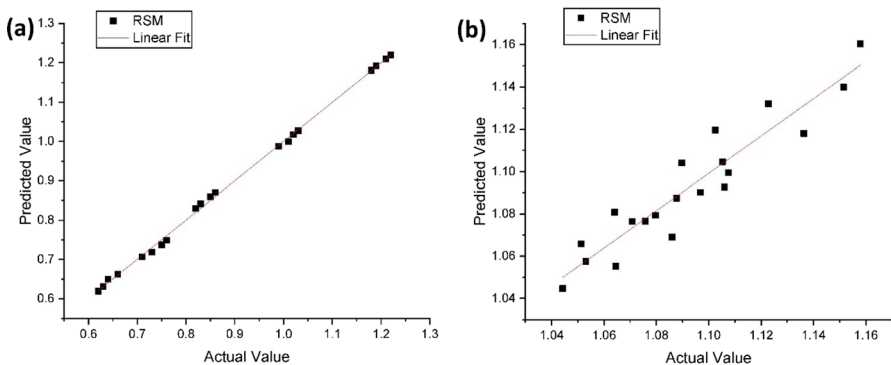


Fig. 9 Linear fitting of RSM predicted value in relation to the experimental data of (a) viscosity and (b) relative viscosity

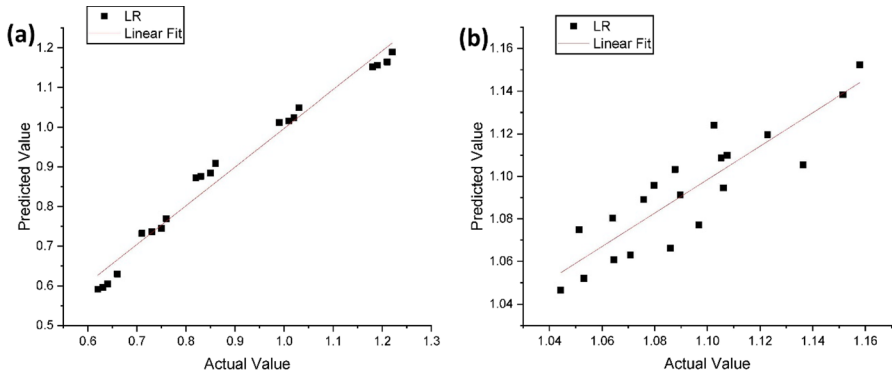


Fig. 10 Linear fitting of LR predicted value in relation to the experimental data of (a) viscosity and (b) relative viscosity

approach, a comparative analysis was performed on their ability to forecast the μ_{nf} and μ_{rel} for numerous applications.

First, an LR analysis was done using the laboratory data, and the resulting correlation model is presented in Eq. (15). The accuracy of the LR model was then evaluated by graphically comparing the predicted and actual values, as shown in Fig. 10a, b. Figure 10a illustrates that the predicted values obtained from the LR model closely matched the actual values of the μ_{nf} , with only a few insignificant outliers. On the other hand, Fig. 10b indicates a more pronounced deviation between the predicted values and actual values of the μ_{rel} compared to that of μ_{nf} . The R -values for the μ_{nf} and μ_{rel} are 0.9881 and 0.8870, respectively. These results suggest that the LR approach can be a useful tool for predicting the properties of GNP-alumina hybrid nanofluids. However, given the limitations of the LR method, such as its inability to capture complex nonlinear relationships [47], this modelling approach will be compared with the ANFIS, ANN and RSM approaches.

Table 9 presents the performance comparison of various models for predicting μ_{nf} and μ_{rel} , while the models' residuals are illustrated in Fig. 11. The models compared are ANFIS, ANN, RSM, and LR. The table presents different performance metrics of the various models used for forecasting the μ_{nf} and μ_{rel} . The metrics include R^2 , MOD, RSS, RMSE, MAE, and MAPE.

A detailed analysis of the results in Table 9 indicates that the ANFIS model consistently demonstrates superior performance across all metrics for both μ_{nf} and μ_{rel} predictions. The R^2 values, which indicate the proportion of variance explained by the model, are notably higher for the ANFIS model than the other models. Additionally, the MOD values for ANFIS are consistently the closest to zero, indicating a better alignment of predicted values with actual values. Furthermore, the ANFIS model exhibits the lowest values for RSS, RMSE, MAE, and MAPE, indicating that it produces predictions with minimal residual errors and high accuracy. This is particularly evident in the significantly lower RMSE and MAE values for the ANFIS model compared to the other models, signifying

Table 9 Performance comparison of the various models

		R^2	Margin of deviation (%)		RSS	RMSE	MAE	MAPE
			Min	Max				
			Viscosity	ANFIS				
	ANN	0.9997	-0.57	1.37	2.65E-04	3.64E-03	2.60E-03	0.3100
	RSM	0.9986	-1.50	1.72	1.10E-03	7.41E-03	5.77E-03	0.7179
	LR	0.9764	-6.34	5.55	1.91E-02	3.09E-02	2.72E-02	3.2167
Relative viscosity	ANFIS	0.9872	-0.89	1.19	2.58E-04	3.59E-03	1.29E-03	0.1214
	ANN	0.9817	-0.33	1.18	4.81E-04	4.90E-03	2.82E-03	0.2588
	RSM	0.8835	-1.57	1.61	2.27E-03	1.06E-02	8.56E-03	0.7814
	LR	0.7868	-2.25	2.71	4.15E-03	1.44E-02	1.16E-02	1.0625

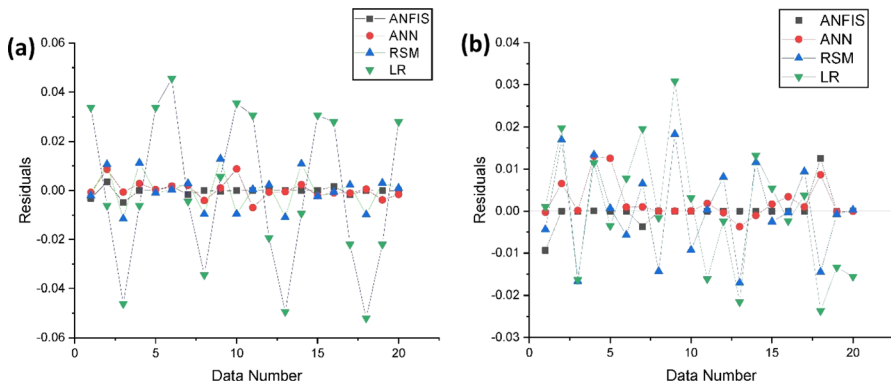


Fig. 11 Residual plot of various predicted data in relation to the experimental data of (a) viscosity and (b) relative viscosity

its ability to make precise predictions. The lower MAPE values highlight the ANFIS model’s capacity to generate predictions with smaller percentage errors.

While the ANN model also performs well across most metrics, the ANFIS model consistently outperforms it. The RSM model, on the other hand, exhibits relatively higher values across the majority of metrics, implying comparatively weaker predictive performance. The LR model consistently fares the poorest among all models, as evidenced by its lower R^2 values and higher errors across the board. The superior predictive capabilities of ANFIS compared to other models and the better performance of ANN relative to RSM and LR align with findings from prior studies [23, 48, 49]. Overall, the results suggest that the ANFIS model could be a better option for predicting μ_{nf} and μ_{rel} values.

4 Conclusion

In this study, the accurate prediction of μ properties for GNP-alumina hybrid nanofluids was investigated through the comparison of various modelling techniques, including RSM, ANN and ANFIS. The study focused on μ_{nf} and μ_{rel} predictions across a wide range of mixing ratios (0, 0.33, 1, and 3) and temperatures (15, 25, 35, 45 and 55 °C). The models were optimised by varying the number of neurons for ANN, while the MF type and MF number were varied for ANFIS. On the other hand, the RSM model's performance was enhanced by varying its source model. The models' performances were estimated using MOD, RSS, RSME, MAE and MAPE.

The findings revealed that the ANN architecture with 4 neurons exhibited exceptional predictive capabilities for μ_{nf} , yielding an impressive R^2 value of 0.9997 and a MAPE of 0.3100. Similarly, for μ_{rel} , the optimal ANN architecture was achieved with 5 neurons, resulting in an R^2 of 0.9817 and a MAPE of 0.2588. The ANFIS model achieved remarkable accuracy, employing PsigMF and DSigMF for μ_{nf} and GBellMF for μ_{rel} , respectively, with (3 5) and (4 5) input membership functions. This was evidenced by R^2 values of 0.9999 and 0.9872, along with corresponding MAPE values of 0.0945 and 0.1214 for the optimal ANFIS architecture of μ_{nf} and μ_{rel} .

Furthermore, the RSM model demonstrated its efficacy in predicting μ properties, specifically with the quadratic model, resulting in R^2 values of 0.9986 and 0.8835 for μ_{nf} and μ_{rel} , respectively. Comparative analysis of the models emphasised the superiority of the ANFIS model in terms of performance metrics for both μ_{nf} and μ_{rel} predictions.

Overall, the results revealed that all the techniques could accurately forecast the μ_{nf} and μ_{rel} of GNP-alumina hybrid nanofluid. Still, the ANN and ANFIS models outperformed the RSM and LR models. This study highlights the potential of ANN and ANFIS models for accurate μ forecasting in GNP-alumina hybrid nanofluids. It provides reliable tools for future applications in a wide array of engineering contexts.

In terms of future research, this study lays the groundwork for further exploration into the interactions between solid volume fractions, mixing ratios, and temperatures on nanofluid behaviour. While this study has focused on the key factors of mixing ratio and temperature in this study, understanding the effects of variations in solid volume fractions on predictive accuracy will be a significant avenue for investigation. Additionally, applying these models to different types of nanoparticles, base fluids, and experimental conditions could provide valuable insights into the broader applicability of the developed predictive tools.

Acknowledgements The authors express their gratitude for the assistance provided by the URC at the University of Johannesburg.

Author contributions AB wrote the main manuscript, and PA reviewed the work, supervised, and contributed resources for work. All authors reviewed the manuscript

Funding Open access funding provided by University of Johannesburg.

Data availability The datasets generated during and/or analysed during the current study are available from the corresponding author on reasonable request.

Declarations

Conflict of interest The authors declare no competing interests.

Open Access This article is licensed under a Creative Commons Attribution 4.0 International License, which permits use, sharing, adaptation, distribution and reproduction in any medium or format, as long as you give appropriate credit to the original author(s) and the source, provide a link to the Creative Commons licence, and indicate if changes were made. The images or other third party material in this article are included in the article's Creative Commons licence, unless indicated otherwise in a credit line to the material. If material is not included in the article's Creative Commons licence and your intended use is not permitted by statutory regulation or exceeds the permitted use, you will need to obtain permission directly from the copyright holder. To view a copy of this licence, visit <http://creativecommons.org/licenses/by/4.0/>.

References

1. Kumar N, Singh P, Redhewal AK, Bhandari P (2015) A review on nanofluids applications for heat transfer in micro-channels. *Procedia Eng* 127:1197–1202. <https://doi.org/10.1016/j.proeng.2015.11.461>
2. Scott TO, Ewim DRE, Eloka-Eboka AC (2022) Hybrid nanofluids flow and heat transfer in cavities: a technological review. *Int J Low-Carbon Technol* 17:1104–1123. <https://doi.org/10.1093/IJLCT/CTAC093>
3. Yang L, Ji W, Mao M, Huang JN (2020) An updated review on the properties, fabrication and application of hybrid-nanofluids along with their environmental effects. *J Clean Prod* 257:120408. <https://doi.org/10.1016/J.JCLEPRO.2020.120408>
4. Borode AO, Ahmed NA, Olubambi PA, Sharifpur M, Meyer JP (2021) Investigation of the thermal conductivity, viscosity, and thermal performance of graphene nanoplatelet-alumina hybrid nanofluid in a differentially heated cavity. *Front Energy Res* 9:482. <https://doi.org/10.3389/fenrg.2021.737915>
5. Hemmat Esfe M, Esfandeh S, Alirezaie A (2017) A novel experimental investigation on the effect of nanoparticles composition on the rheological behavior of nano-hybrids. *J Mol Liq*. <https://doi.org/10.1016/j.molliq.2017.11.147>
6. Khan MS, Abid M, Ali HM, Amber KP, Bashir MA, Javed S (2019) Comparative performance assessment of solar dish assisted s-CO₂ Brayton cycle using nanofluids. *Appl Therm Eng* 148:295–306. <https://doi.org/10.1016/J.APPLTHERMALENG.2018.11.021>
7. Khodadadi H, Aghakhani S, Majd H, Kalbasi R, Wongwises S, Afrand M (2018) A comprehensive review on rheological behavior of mono and hybrid nanofluids: effective parameters and predictive correlations. *Int J Heat Mass Transf* 127:997–1012. <https://doi.org/10.1016/j.ijheatmasstransfer.2018.07.103>
8. Aybar H, Sharifpur M, Azizian MR, Mehrabi M, Meyer JP (2015) A review of thermal conductivity models for nanofluids. *Heat Transf Eng* 36(13):1085–1110. <https://doi.org/10.1080/01457632.2015.987586>
9. Hemmat Esfe M, Bahiraei M, Mahian O (2018) Experimental study for developing an accurate model to predict viscosity of CuO–ethylene glycol nanofluid using genetic algorithm based neural network. *Powder Technol* 338:383–390. <https://doi.org/10.1016/J.POWTEC.2018.07.013>
10. Malika M, Sonawane SS (2021) Application of RSM and ANN for the prediction and optimization of thermal conductivity ratio of water based Fe₂O₃ coated SiC hybrid nanofluid. *Int Commun Heat Mass Transf* 126:105354. <https://doi.org/10.1016/J.ICHEATMASSTRANSFER.2021.105354>
11. Baghban A, Kahani M, Nazari MA, Ahmadi MH, Yan WM (2019) Sensitivity analysis and application of machine learning methods to predict the heat transfer performance of CNT/water nanofluid flows through coils. *Int J Heat Mass Transf* 128:825–835. <https://doi.org/10.1016/J.IJHEATMASSTRANSFER.2018.09.041>

12. Alade IO, Abd Rahman MA, Saleh TA (2019) Modeling and prediction of the specific heat capacity of Al_2O_3 /water nanofluids using hybrid genetic algorithm/support vector regression model. *Nano-Struct Nano-Objects* 17:103–111. <https://doi.org/10.1016/J.NANOSO.2018.12.001>
13. Alhadri M, Raza J, Yashkun U et al (2022) Response surface methodology (RSM) and artificial neural network (ANN) simulations for thermal flow hybrid nanofluid flow with Darcy-Forchheimer effects. *J Indian Chem Soc* 99(8):100607. <https://doi.org/10.1016/J.JICS.2022.100607>
14. Hemmat Esfe M, Hassani Ahangar MR, Rejvani M, Toghraie D, Hajmohammad MH (2016) Designing an artificial neural network to predict dynamic viscosity of aqueous nanofluid of TiO_2 using experimental data. *Int Commun Heat Mass Transf* 75:192–196. <https://doi.org/10.1016/j.icheatmasstransfer.2016.04.002>
15. Shahsavari A, Khanmohammadi S, Toghraie D, Salihepour H (2019) Experimental investigation and develop ANNs by introducing the suitable architectures and training algorithms supported by sensitivity analysis: measure thermal conductivity and viscosity for liquid paraffin based nanofluid containing Al_2O_3 nanoparticles. *J Mol Liq* 276:850–860. <https://doi.org/10.1016/J.MOLLIQ.2018.12.055>
16. Afrand M, Ahmadi Nadooshan A, Hassani M, Yarmand H, Dahari M (2016) Predicting the viscosity of multi-walled carbon nanotubes/water nanofluid by developing an optimal artificial neural network based on experimental data. *Int Commun Heat Mass Transf* 77:49–53. <https://doi.org/10.1016/J.ICHEATMASSTRANSFER.2016.07.008>
17. Mehrabi M, Sharifpur M, Meyer JP (2013) Viscosity of nanofluids based on an artificial intelligence model. *Int Commun Heat Mass Transf* 43:16–21. <https://doi.org/10.1016/J.ICHEATMASSTRANSFER.2013.02.008>
18. Çolak AB (2021) A novel comparative analysis between the experimental and numeric methods on viscosity of zirconium oxide nanofluid: developing optimal artificial neural network and new mathematical model. *Powder Technol* 381:338–351. <https://doi.org/10.1016/J.POWTEC.2020.12.053>
19. Toghraie D, Sina N, Jolfaei NA, Hajian M, Afrand M (2019) Designing an artificial neural network (ANN) to predict the viscosity of silver/ethylene glycol nanofluid at different temperatures and volume fraction of nanoparticles. *Phys A Stat Mech Its Appl* 534:122142. <https://doi.org/10.1016/J.PHYSA.2019.122142>
20. Bhat AY, Qayoum A (2022) Viscosity of CuO nanofluids: experimental investigation and modeling with FFBP-ANN. *Thermochim Acta* 714:179267. <https://doi.org/10.1016/j.tca.2022.179267>
21. Esfe MH, Khaje Khabaz M, Esmaily R et al (2022) Application of artificial intelligence and using optimal ANN to predict the dynamic viscosity of hybrid nano-lubricant containing zinc oxide in commercial oil. *Colloids Surf A Physicochem Eng Asp* 647:129115. <https://doi.org/10.1016/j.colsurfa.2022.129115>
22. Hemmat Esfe M, Hajian M, Toghraie D et al (2022) Prediction the dynamic viscosity of MWCNT- Al_2O_3 (30:70)/ Oil 5W50 hybrid nano-lubricant using principal component analysis (PCA) with artificial neural network (ANN). *Egypt Inform J* 23(3):427–436. <https://doi.org/10.1016/j.eij.2022.03.004>
23. Khetib Y, Abo-Dief HM, Alanazi AK, Rawa M, Sajadi SM, Sharifpur M (2021) Competition of ANN and RSM techniques in predicting the behavior of the CuO-liquid paraffin. *Chem Eng Commun* 210(6):880–892. <https://doi.org/10.1080/00986445.2021.1980398>
24. Qing H, Hamed S, Eftekhari SA et al (2021) A well-trained feed-forward perceptron artificial neural network (ANN) for prediction the dynamic viscosity of Al_2O_3 -MWCNT (40:60)-Oil SAE50 hybrid nano-lubricant at different volume fraction of nanoparticles, temperatures, and shear rates. *Int Commun Heat Mass Transf* 128:105624. <https://doi.org/10.1016/j.icheatmasstransfer.2021.105624>
25. Borode AO, Ahmed NA, Olubambi PA (2021) Electrochemical corrosion behavior of copper in graphene-based thermal fluid with different surfactants. *Heliyon* 7(1):e05949. <https://doi.org/10.1016/j.heliyon.2021.e05949>
26. Khdher AM, Sidik NAC, Hamzah WAW, Mamat R (2016) An experimental determination of thermal conductivity and electrical conductivity of bio glycol based Al_2O_3 nanofluids and development of new correlation. *Int Commun Heat Mass Transf* 73:75–83. <https://doi.org/10.1016/J.ICHEATMASSTRANSFER.2016.02.006>
27. Çolak AB (2022) Analysis of the effect of arrhenius activation energy and temperature dependent viscosity on non-newtonian maxwell nanofluid bio-convective flow with partial slip by artificial

- intelligence approach. *Chem Thermodyn Therm Anal* 6:100039. <https://doi.org/10.1016/j.ctta.2022.100039>
28. Braspenning PJ, Thuijsman F, Weijters A (1995) Artificial neural networks: an introduction to ANN theory and practice. *Psicothema* 931:293. Accessed 17 March 2023. <http://www.ncbi.nlm.nih.gov/pubmed/22047867>
 29. Bahiraei M, Nazari S, Moayedi H, Safarzadeh H (2020) Using neural network optimized by imperialist competition method and genetic algorithm to predict water productivity of a nano-fluid-based solar still equipped with thermoelectric modules. *Powder Technol* 366:571–586. <https://doi.org/10.1016/J.POWTEC.2020.02.055>
 30. Toghraie D, Sina N, Mozafarifard M, Alizadeh A, Soltani F, Fazilati MA (2020) Prediction of dynamic viscosity of a new non-newtonian hybrid nanofluid using experimental and artificial neural network (ANN) methods. *Heat Transf Res* 51(15):1351–1362. <https://doi.org/10.1615/HEATTRANSRES.2020034645>
 31. Yang X, Boroomandpour A, Wen S, Toghraie D, Soltani F (2021) Applying artificial neural networks (ANNs) for prediction of the thermal characteristics of water/ethylene glycol-based mono, binary and ternary nanofluids containing MWCNTs, titania, and zinc oxide. *Powder Technol* 388:418–424. <https://doi.org/10.1016/J.POWTEC.2021.04.093>
 32. Luo N, Yu H, You Z et al (2023) Fuzzy logic and neural network-based risk assessment model for import and export enterprises: a review. *J Data Sci Intell Syst* 1(1):2–11. <https://doi.org/10.47852/bonviewJDSIS32021078>
 33. Abonyi J, Andersen H, Nagy L, Szeifert F (1999) Inverse fuzzy-process-model based direct adaptive control. *Math Comput Simul* 51(1):119–132. [https://doi.org/10.1016/S0378-4754\(99\)00142-1](https://doi.org/10.1016/S0378-4754(99)00142-1)
 34. Babanezhad M, Nakhjiri AT, Shirazian S (2020) Changes in the number of membership functions for predicting the gas volume fraction in two-phase flow using grid partition clustering of the ANFIS method. *ACS Omega* 5(26):16284–16291. <https://doi.org/10.1021/acsomega.0c02117>
 35. Salleh MNM, Talpur N, Talpur KH (2018) A modified neuro-fuzzy system using metaheuristic approaches for data classification. *IntechOpen*
 36. El-Haik KYB, Yang K (2003) Design for six sigma a roadmap for product development. RR Donnelly
 37. Myers RH, Montgomery DC, Anderson-Cook CM (2016) Response surface methodology: process and product optimization using designed experiments. John Wiley & Sons
 38. Yashawantha KM, Vinod AV (2021) ANFIS modelling of effective thermal conductivity of ethylene glycol and water nanofluids for low temperature heat transfer application. *Therm Sci Eng Prog* 24:100936. <https://doi.org/10.1016/j.tsep.2021.100936>
 39. Syam Sundar L, Sambasivam S, Mewada HK (2022) ANFIS modelling with fuzzy C-mean clustering of experimentally evaluated thermophysical properties of zirconia-water nanofluids. *J Mol Liq* 364:119987. <https://doi.org/10.1016/j.molliq.2022.119987>
 40. Amiri A, Shanbedi M, Dashti H (2017) Thermophysical and rheological properties of water-based graphene quantum dots nanofluids. *J Taiwan Inst Chem Eng* 76:132–140. <https://doi.org/10.1016/j.jtice.2017.04.005>
 41. Bahrami M, Akbari M, Karimipour A, Afrand M (2016) An experimental study on rheological behavior of hybrid nanofluids made of iron and copper oxide in a binary mixture of water and ethylene glycol: non-Newtonian behavior. *Exp Therm Fluid Sci* 79:231–237. <https://doi.org/10.1016/J.EXPTHERMFLUSCI.2016.07.015>
 42. Dezfulizadeh A, Aghaei A, Joshaghani AH, Najafizadeh MM (2021) An experimental study on dynamic viscosity and thermal conductivity of water-Cu-SiO₂-MWCNT ternary hybrid nanofluid and the development of practical correlations. *Powder Technol* 389:215–234. <https://doi.org/10.1016/J.POWTEC.2021.05.029>
 43. Borode AO, Ahmed NA, Olubambi PA (2019) Application of carbon-based nanofluids in heat exchangers: current trends. *J Phys Conf Ser* 1378:032061. <https://doi.org/10.1088/1742-6596/1378/3/032061>
 44. Yu L, Bian Y, Liu Y, Xu X (2019) Experimental investigation on rheological properties of water based nanofluids with low MWCNT concentrations. *Int J Heat Mass Transf* 135:175–185. <https://doi.org/10.1016/j.ijheatmasstransfer.2019.01.120>
 45. Goodarzi M, Toghraie D, Reiszadeh M, Afrand M (2019) Experimental evaluation of dynamic viscosity of ZnO-MWCNTs/engine oil hybrid nanolubricant based on changes in temperature

- and concentration. *J Therm Anal Calorim* 136(2):513–525. <https://doi.org/10.1007/S10973-018-7707-8/FIGURES/10>
46. Yan SR, Kalbasi R, Nguyen Q, Karimipour A (2020) Rheological behavior of hybrid MWCNTs-TiO₂/EG nanofluid: a comprehensive modeling and experimental study. *J Mol Liq* 308:113058. <https://doi.org/10.1016/J.MOLLIQ.2020.113058>
 47. Huo S, He Z, Su J, Xi B, Zhu C (2013) Using artificial neural network models for eutrophication prediction. *Procedia Environ Sci* 18:310–316. <https://doi.org/10.1016/J.PROENV.2013.04.040>
 48. Chu YM, Ibrahim M, Saeed T, Berrouk AS, Algehyne EA, Kalbasi R (2021) Examining rheological behavior of MWCNT-TiO₂/5W40 hybrid nanofluid based on experiments and RSM/ANN modeling. *J Mol Liq* 333:115969. <https://doi.org/10.1016/J.MOLLIQ.2021.115969>
 49. Igwilo CN, Ude NC, Onoh IM, Enekwe CB, Alieze BA (2022) RSM, ANN and ANFIS applications in modeling fermentable sugar production from enzymatic hydrolysis of *Colocynthis Vulgaris* Shrad seeds shell. *Bioresour Technol Rep* 18:101056. <https://doi.org/10.1016/J.BITEB.2022.101056>

Publisher's Note Springer Nature remains neutral with regard to jurisdictional claims in published maps and institutional affiliations.

Authors and Affiliations

Adeola Borode¹ · Peter Olubambi¹

✉ Adeola Borode
hadeyola2003@yahoo.com; aborode@uj.ac.za

¹ Centre for Nanoengineering and Advanced Materials, School of Mining, Metallurgical and Chemical Engineering, University of Johannesburg, Johannesburg, Doornfontein, South Africa